ACS OMEGA

Open Access

http://pubs.acs.org/journal/acsodf

Article

Crystallinity Reconstruction of Squid-Pen Chitosan into Mechanically Robust and Multifunctional Bionanocomposite Food Packaging Film

Nattapong Pinpru,[§] Chiranicha Ninthap,[§] and Varol Intasanta*

Cite This: *ACS Omega* 2024, 9, 41179–41193

Read Online

ACCESS | Metrics & More | Article Recommendations | Supporting Information

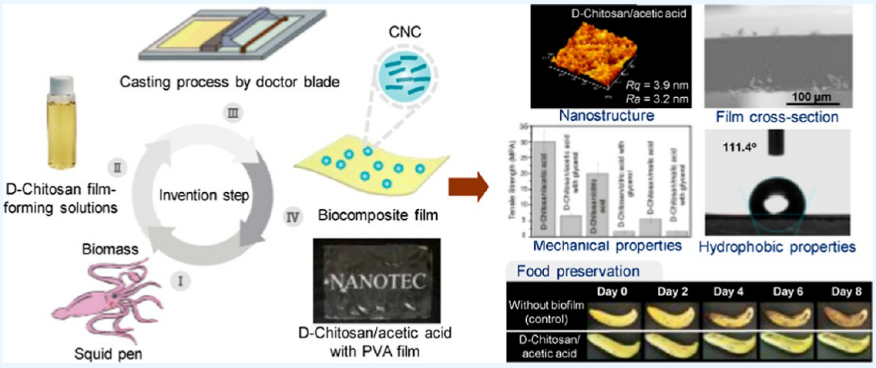

ABSTRACT: First, we explore the effect of bioacids on the film processing of preprocessed, i.e., deacetylated, chitosan (D-chitosan with molecular weight of 1,000,000 kDa), using monocarboxylic acid (acetic acid), dicarboxylic acid (malic acid), and tricarboxylic acid (citric acid) as model weak acidic solvents to destabilize the hydrogen bonding and transform crystal structures into film. Second, we investigate the chemical and physical toughening effect in the bionanocomposite film composed of cross-linkable multicarboxilic acid, i.e., succinic acid (SA). In doing so, the addition of glycerol as a plasticizer can increase polymer chain mobility, making the biocomposite film more ductile and flexible. The addition of CNC also enhances the tensile strength (41.6%), swelling (43.47%), and oxygen barrier properties (38.81%), as well as significantly improves UV light barrier. The excellent antibacterial properties (99.9% efficiency against *S. aureus* and *K. pneumoniae*) of the prepared biocomposite films are found to be independent of the presence of glycerol or CNC. Third, the development of film processability under an industrially relevant process is also demonstrated by doctor blade method. It is found that film processability of the squid-pen's chitosan bionanocomposite can straightforwardly be compatible with and improvable in the presence of poly(vinyl alcohol) employed as a model biodegradable processing aid.

1. INTRODUCTION

The food packaging film industry is increasingly threatening to our environment because of the single-use and nondegradable plastics, including low-density polyethylene (LDPE), linear low-density polyethylene, high-density polyethylene, and polypropylene (PP), to name a few.[1] These plastics, while producing a large amount of garbage on the surface of the Earth and being a major source of greenhouse gas emissions, which inevitably contribute to global warming, have a noticeable negative influence on the environment, which includes humans, plants, and animals.[2] Nevertheless, shifting from nondegradable and petro-based film into biodegradable film is no easy task, where the challenge lies among properties, cost, and scalability of the new venture. As of current demand, the film employed must be capable of protecting food from the environment, particularly from bacteria and air pollution, extending the shelf life required for storage and transportation. In particular, films that are effective and suited for food packaging should be of sufficient strength, have low oxygen permeability (OP), and be nontoxic to food. Therefore, to help the world and the environment, it is vital to develop novel biofilm plastics that are both environmentally benign and functional for food packaging applications. While the biobased film derived solely from petrochemicals such as poly(vinyl alcohol) (PVA), polylactic acid, and polybutylene succinate (PBS) are biodegradable and so attractive as plastic alternatives, their sole use currently raises some serious concerns. These concerns are tremendous carbon dioxide

Received: February 15, 2024
Revised: September 12, 2024
Accepted: September 18, 2024
Published: September 24, 2024

release upon fabrication, high cost for industrial production,[3] and limited supply of raw materials. Thus, it is of considerable interest to develop a mechanically robust and functional bioplastic film from abundantly available natural and biodegradable materials.

Chitosan is a linear polysaccharide made up of β-(1 → 4)-linked D-glucosamine (deacetylated unit) and *N*-acetyl-D-glucosamine (acetylated unit) dispersed randomly.[4] The biopolymer is a deacetylated derivative of chitin that can be found in crustacean shells, insects, fungus, to name a few.[5] Chitosan has a wide range of intriguing properties, including antimicrobial activity, biocompatibility, biodegradability, and nontoxicity.[6]

Composed primarily of chitin, the gladius or pen is a hard but flexible internal structure found in many cephalopods, such as squids in particular. Abundant as waste from fishery worldwide, squid-pen represents a unique class of mechanically robust, bionanostructural, and semicrystalline biomass. Chitosan derived from squid pens' chitin has a β-structure, which means that the polymer chains are arranged in parallel directions and held together by weak intrasheet intermolecular hydrogen bonding.[7] Chitosan derived from animal shells, on the other hand, has an α-structure that aligns in an antiparallel pattern with strong intra- and intersheet hydrogen bonding.[8] β-chitosan outperformed others to form structures in terms of antibacterial activity and mechanical strength.[9] Furthermore, chitosan derived from squid pens shows better solubility, reactivity, solvent affinity, and swelling than other chitosan-forming structures.[10] Among film fabrication technologies, solvent casting is one of the most versatile and cost-effective methods involving low-temperature and solution-based processing and thus suitable for temperature-sensitive biomaterials. Due to its strong hydrogen bonding and crystallinity, an acidic solution is required to dissolve the chitosan in this method. Most bioacids used for dissolving and producing biofilms from chitosan are carboxylic acids,[11] in three forms: monocarboxylic, dicarboxylic, and tricarboxylic acids.[12] Monocarboxylic acids such as acetic and formic acids are usually used to dissolve chitosan to produce biofilms, because of their low cost and nontoxicity. Dicarboxylic acids, such as malic and sebacic acids, are less common for dissolving chitosan for biofilm formation due to their low chitosan solubility. And then, tricarboxylic acids such as citric and trimesic acids have been employed to dissolve chitosan and produce biofilms, but they are not widely used. However, these acids are unsatisfactory in producing films from chitosan, particularly in terms of the mechanical properties. In addition, no substantial investigation on the efficiency of biofilms has been published to evaluate which biobased carboxylic acids are most fit for solution-based biofilm formation from chitosan derived from the chemically and mechanically unique squid pens' chitin with the β-structure.

Nonetheless, most biopolymer films have disadvantages when compared to olefin films, such as low mechanical properties or even film stability. As a result of this disadvantage, biopolymer packaging film is frequently difficult to employ since it affects food shelf life. To overcome these drawbacks, forming a biobased film and toughening it via both chemical and physical approaches to improve its properties would be a viable strategy to optimize the film. In the physical approach, studying biofilms made of chitosan dissolved in different acids and increasing their effectiveness with fillers have both been the subjects of extensive investigation. Velasquez-Cock et al. developed chitosan biofilms from acetic and lactic acids, resulting in biofilms with excellent bacterial resistance.[13] Nevertheless, the strength was low; thus, the biofilms were reinforced with bacterial nanocellulose to improve their strength. Brink et al. (2019) used acetic acid to produce chitosan biofilms that were reinforced with whey protein, resulting in greater film strength but too fast degradation.[14] In particular, Costa et al. (2021) produced chitosan/cellulose nanocrystal (CNC) biofilms to improve tensile strength (TS) and lower oxygen barrier values, as well as extend shelflife of the biofilms.[15]

In that respect, cellulose is a linear polymer glucan composed of more than 10,000 glucose molecules linked by β-(1−4)-glycosidic bonds.[16] It is typically produced by plants, but some bacteria, such as *Acetobacter xylinum*, can also produce it.[16] Cellulose is widely used in a range of industries, including clothing, paper, and leather, due to its low cost and easy availability.[17] Cellulose particle sizes range from micrometers to nanometers, with the nanosize being more beneficial in specialized industries because it improves the stability of the material. Cellulose nanocrystals (CNCs) have a low density, are light in weight, and are inexpensive when compared to other nanofillers.[18] It also enhances the mechanical properties of the material, particularly the film, and is very safe to use with a food packaging film. More importantly, it decomposes quickly when exposed to microorganisms in the environment, so it does not generate waste. Furthermore, when the potential of nano- and micron-sized cellulose were compared, it was discovered that nanosize appeared to be outstanding in all dimensions of application to film materials.[19] In that spirit, a considerable amount of research has been performed to investigate different types of chitosan composite films. de Mesquita et al. incorporated a 145 nm long and 6 nm diameter *n*-cellulose crystal into a chitosan matrix and found the film to be strong and durable.[20] Fernandes et al. created chitosan/nanocellulose composite films using low and high molecular weight chitosan powders and studied the mechanical and thermal properties of the composites, finding that adding nanocellulose enhanced the breakdown temperature of chitosan films by up to 45 °C.[21]

In the chemical route, forming molecular cross-linking networks could be of scientific novelty. For example, succinic acid (SA) is regarded as a potential chitosan solvent not only for its ability to protonate the amine group but also for its inherent biodegradability and nonbioaccumulation.[22] SA is inexpensive since it is easily manufactured using biological processes.[22] SA is a dicarboxylic acid with the formula $(CH_2)_2(CO_2H)_2$, and its molecular chain contains a variety of active functional groups that can react with a wide range of organic compounds, including amino and polysaccharide groups.[23] SA has the ability to improve the physical and chemical properties of some biopolymers, such as chitosan and gelatin, as well as enhance polymer crystallinity.[24] Furthermore, dicarboxylic acids as SA could behave as ionic cross-linkers between chitosan molecules, which has been shown that when dicarboxylic acid replaces acetic acid or inorganic acids, mechanical properties are greatly improved.[25]

In this work, the ultimate objective is to develop a chitosan-based and bionanocomposite food packaging film from a squid pen as a model starting material with chitin of the β-structure. First, we explored the effect of bioacids on the film processing of preprocessed, i.e., deacetylated, chitosan (D-chitosan), using monocarboxylic acid (acetic acid), dicarboxylic acid (malic acid), and tricarboxylic acid (citric acid) as weak acidic solvents to destabilize the hydrogen bonding and transform crystal structures into film via facile solvent casting. Upon property

https://doi.org/10.1021/acsomega.4c01482
ACS Omega 2024, 9, 41179−41193

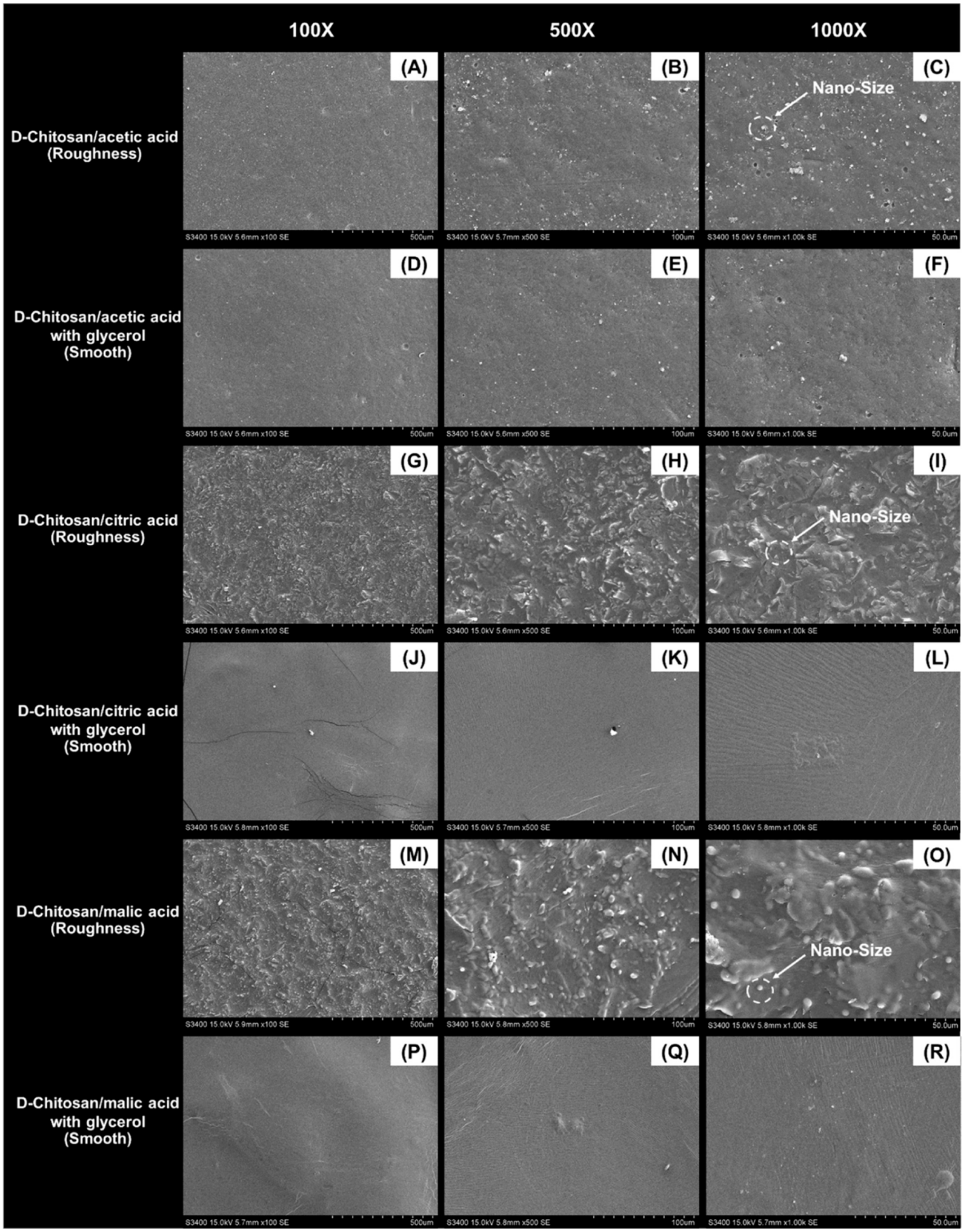

Figure 1. Morphology of biofilms under magnifications of 100×, 500×, and 1000×.

verification, the potential of biofilms was evaluated by wrapping Cavendish bananas to study their practical ability to extend the shelf life. Second, we further investigated the toughening effect, both chemical and physical, in the bionanocomposite film composed of cross-linkable multicarboxilic acid, i.e., succinic acid (SA) as model bioacid and cellulose nanocrystal as a model nanofiller. Finally, we investigated the possibility of developing film processability under an industrially relevant process, i.e., doctor blade, to validate the research's potential toward real-world applications.

2. MATERIALS AND METHODS

2.1. Materials. Chitosan extract from squid pen, 95% degree of deacetylation, having a molecular weight of 1,000,000 kDa, was supplied by Bonafides Marketing Co., Ltd. (Bangkok,

https://doi.org/10.1021/acsomega.4c01482
ACS Omega 2024, 9, 41179−41193

Thailand). Acetic acid (CH_3COOH; purity 99.5%, analytical grade), citric acid ($C_6H_8O_7$; purity 99.2%, analytical grade), and malic acid ($C_4H_6O_5$; purity 99.5%, analytical grade) were purchased from Sigma-Aldrich. Glycerol (minimum assay: 97.4%, analytical grade) was purchased from Chemipan Co., Ltd. (Bangkok, Thailand). Succinic acid (SA; purity 99.5%, analytical grade) and cellulose nanocrystals (CNC; purity 99.2%, analytical grade with 10−20 nm diameters) were purchased from Sigma-Aldrich. Deionized water (DW; pH 7.12) was prepared in our laboratories by distillation.

2.2. Film Preparation. *2.2.1. D-Chitosan in Bioacid.* First, 2% w/v of D-chitosan solution was prepared by dissolving D-chitosan powder in an aqueous solution of 2% w/v of various acids (acetic, citric, and malic acid) under continuous stirring for 6 h. After that, 0.5 mL of glycerol was added. Subsequently, these solutions were left under constant stirring for 1 h, homogenized, and then cooled to room temperature to remove air bubbles. Finally, the solutions were cast into a rectangular container. After being cast, the biofilms were dried at 70 °C for 12 h.

2.2.2. D-Chitosan in SA and D-Chitosan with CNC in SA. First, 2% w/v SA aqueous solution was made by dissolving 2 g of SA in 100 mL of deionized water with continuous stirring at 90 °C. Then, a 2% w/v chitosan solution in SA was made by dissolving 2 g of chitosan powder in 100 mL of the 2% w/v SA aqueous solution with 6 h of continuous stirring at 90 °C. Then 0.5 mL of glycerol was added to the above mixture. Subsequently, varying CNC quantities were added (0 and 0.5 wt % based on chitosan weight) to the above mixture. After 1 h of constant stirring at 90 °C, these solutions were homogenized and cooled to room temperature to remove the air bubbles. Finally, the solutions were poured into a rectangular container. The biocomposite films were cast and dried for 12 h at 70 °C. Figure 1 depicts the preparation of the biocomposite films.

2.3. Solution Properties. The studies on solution conductivity were carried out using a Malvern Zetasizer Nano-ZS. The solutions were loaded into a disposable capillary cell, and the measurement was performed at room temperature. The viscosity of the solutions was examined using a Brookfield DV-IIV ultra programmable rheometer equipped with a CPA-40Z cone and plate geometry spindle at room temperature. All the data reported was collected in triplicate and averaged.

2.4. Mechanical Properties. TS and elongation at break (EB) of biofilms were determined, following ASTM standard method D882-18 (2018), using a Universal Testing Machine (Instron model 5566) at room temperature with 48 ± 5% relative humidity. Ten 10 mm × 70 mm film samples, with an initial grip length of 50 mm, were used. Each biofilm was clamped and deformed under tensile loading using a 50 N load cell with a cross-head speed of 30 mm/min until the samples were broken. The maximum load and the final extension at break were used to calculate the TS and EB.

2.5. Morphology by SEM. A scanning electron microscope (SEM) (Hitachi S-3400N) was used to investigate the surface morphologies of biofilms. Samples were coated with a thin layer of gold. The images of the samples were magnified and digitally recorded. An accelerated voltage of 5 kV was used as the operating condition.

2.6. Fourier Transforms Infrared Spectroscopy Analysis. Fourier transforms infrared spectroscopy (FT-IR) spectra in the transmission mode of D-chitosan and biofilms were recorded by using a Nicolet 6700 spectrometer (Thermo Scientific) with a resolution of 4 cm^{-1} in a spectral range of 4000−700 cm^{-1} with 64 scans per sample at room temperature.

2.7. Optical Microscope Analysis. A Nikon Eclipse LV150 camera was used to photograph the crystallinity of the biocomposite films. Images of optical microscopy were captured using a microcapture recorder system at room temperature.

2.8. Crystal Structure Analysis. The crystal structure of D-chitosan and biofilms were recorded using an X-ray Diffractometer (model D8 Advance), using silicon as base reference. The measurement mode was Cu Kα with 40 kV. The samples were studied over a diffraction range of 2θ about 10−60° with a step size of 0.02° at 25 °C. The percent of crystallinity was calculated as the following equation

$$\%\ \text{crystallinity} = \frac{\text{area of the crystallinity}}{\text{total area of peaks}} \times 100 \quad (1)$$

2.9. Swelling Properties. The swelling ratio (SR) of the biofilms was measured by using the gravimetric method. A known weight of the dry film was soaked in 100 mL of deionized water for 60 min. Then, the water in the container was separated from the swollen biofilm using a paper filter. The swollen film was then weighed and the SR was determined from

$$\text{SR} = \frac{(M_s - M_d)}{M_d} \quad (2)$$

where M_d and M_s represent mass of dried and swollen films, respectively.

2.10. Contact Angle Analysis. Contact angle analysis was carried out using a Dataphysics brand tension meter, model PSL 250. The 5 × 5 cm^2 size of the sample was wetted with 2 μL of DI water. Evaluations were carried out every 1 s. Since DI water represented a model hydrophilic media, the contact angles of lower than 90° indicated the hydrophilic nature of the test surface, whereas the values higher than 90° suggested the hydrophobic property.

2.11. OP Analysis. The determination of the O_2 transmission was conducted by the differential-pressure method using a VAC-V1 Gas Transmission Tester (Shimizu, Japan) according to the national standard of the ASTM standard method D3985 (2020). The tests were carried out at 23 °C in a dry (0% RH) environment.

2.12. Antibacterial Against. The antibacterial property of the biofilm was measured according to the standard of AATCC 100 (2012). A specimen of each biofilm (about 5 g) was transferred to a flask; 1.0 ± 0.1 mL of the inoculum was added to each specimen. All flasks were incubated at 37 °C for 1 h (contact time). After incubation, 100 ± 1 mL of a buffer solution at pH 7 was added to each flask, and the mixture was shaken vigorously for 1 min. A total of 1.0 ± 0.1 mL of the solution was diluted 1:10 in the same buffer solution. 1.0 ± 0.1 mL of the diluted solution was plated on nutrient agar. The inoculated plates were incubated at 37 °C for 24 h, and the surviving colonies were counted. Equation 3 was used to calculate the reduction (%) for *S. aureus* and *K. pneumoniae*.

$$\%\ \text{Reduction}(R) = \frac{100 \times (C - A)}{C} \quad (3)$$

where A is the number of bacteria (cfu/sample) recovered from the inoculated treated test specimen swatches in the jar after 24 h contact time. C is the number of bacteria (cfu/sample) recovered from the inoculated untreated control swatches in the jar at 0 h contract time.

2.13. UV-Light Barrier Properties. UV light barrier properties were tested in the UV−visible (VIS) spectral region

https://doi.org/10.1021/acsomega.4c01482
ACS Omega 2024, 9, 41179−41193

by using a spectrophotometer (Agilent Technologies Model Carry 5000) in transmission mode. The light-barrier properties of the biocomposite film could be evaluated, based on the spectral plots and transmittance values.

2.14. Atomic Force Microscopy Analysis. Atomic force microscopy (AFM) was performed on the D-chitosan film's surface under the tapping mode using the Hitachi research-grade atomic force microscope, model AFM5300E. From the high image, surface topology and side-view roughness could be analyzed.

2.15. Differential Scanning Calorimetry Analysis. Differential scanning calorimetry (DSC) measurements were conducted on D-chitosan films using a Shimadzu/DSC-60A Plus. The temperature range for the measurements was from −50 to 350 °C, with a heating and cooling rate of 10 °C/min under a nitrogen atmosphere at a flow rate of 50 mL/min^{-1}.

2.16. Thermogravimetric Analysis. Thermogravimetric analysis (TGA) was performed on D-chitosan films using a Shimadzu/DTG-60AH. Each analysis utilized 5 mg of the sample, and the temperature range for the analysis was 25−800 °C, with a heating and cooling rate of 10 °C/min under a nitrogen atmosphere at a flow rate of 50 mL/min^{-1}.

2.17. Statistical Analysis. Data analysis was performed with the SPSS software system (Origin Pro 8.0, version 2020, USA). Each experiment was repeated at least three times. A one-way analysis of variance was performed on the experimental data. The mean comparisons were run by Duncan's multiple-range test with the level of significance set at $p \ll 0.05$.

3. RESULTS AND DISCUSSION

3.1. Part 1: Effect of Bioacids on Squid-Pen Chitosan Solution and Film Processability. *3.1.1. Visual Appearance of the D-Chitosan Film-Forming Solution.* As summarized in Table 1, the film-forming solution was made at a low temperature. As a result, it uses less energy and is more environmentally friendly. The homogeneous dispersion of glycerol in the multicarboxylic acid solution and the stirring of the D-chitosan formed a substantial amount of foam. When the solution was cooled to room temperature, the foam was easily removed, leaving a clear solution free of air bubbles. Figure S1 shows that D-chitosan film-forming solutions were indeed relatively transparent when dissolved in acetic acid (Figure S1A), citric acid (Figure S1C), and malic acid (Figure S1E). Meanwhile, there was no apparent shift in color when glycerol was added to the D-chitosan/multicarboxylic acid solution (Figure S1B,D,F) because glycerol is clear and colorless, it has no effect on the color change of the solution. Therefore, all D-chitosan solution formulations provide the same color characteristics.

Table 1. Viscosity and Conductivity of D-Chitosan Solutions with Bioacid at 25 °C

solutions	solution properties	
	viscosity (cP)[a]	conductivity (μS/cm)[a]
D-chitosan/acetic acid	50.77 ± 2.41	1237.56 ± 6.00
D-chitosan/acetic acid with glycerol	72.96 ± 3.22	1217.13 ± 6.95
D-chitosan/citric acid	106.30 ± 3.56	3010.83 ± 13.26
D-chitosan/citric acid with glycerol	127.40 ± 3.38	2961.47 ± 5.83
D-chitosan/malic acid	293.39 ± 4.12	3084.80 ± 1.82
D-chitosan/malic acid with glycerol	303.30 ± 3.67	3018.90 ± 13.37

[a]Mean of three replicates ± standard deviations.

3.1.2. Solution Properties. D-Chitosan powder was soluble in an aqueous solution of acetic, citric, and malic acids. The solution characteristics of viscosity and conductivity were noticeably varying at the same concentration of D-chitosan (2 wt %) in a multicarboxylic acid solvent with a different formula. These two parameters are important for determining the film ability and morphology throughout the solvent casting process. Table 1 shows the viscosity and conductivity of D-chitosan solutions. The viscosity of the D-chitosan/multicarboxylic acid solution ranges from 50.77 to 303.30 cP (Table 1), which is a high viscosity value when compared to water (1 cP at 25 °C by ASTM D445). This demonstrated the presence of chain-to-chain D-chitosan polymer entanglement in the multicarboxylic acid solution.[26] When glycerol was added to a D-chitosan/multicarboxylic acid solution, the viscosity increased significantly. This could be explained by the combination solution being more sticky and forming a dense network solution.[21] Thus, an increase in viscosity could be explained by an enhancement in the polymer−solvent interaction behavior. Furthermore, this research revealed that D-chitosan in acetic acid had a viscosity lower than that of citric and malic acids. This is considered to be a result of its excellent solubility and compatibility with the D-chitosan powder. Therefore, the high compatibility between acetic acid and D-chitosan has an effect on the film properties. For conductivity measurement, the conductivity of D-chitosan solutions in multicarboxylic acid ranges from 1217 to 3084 μS/cm (Table 1). The values are very high because the effect in conductivity could be due to a significant ionic interaction in the solution between NH^{3+} and COO^{-} of D-chitosan and multicarboxylic acid.[27] When glycerol was added to the D-chitosan/multicarboxylic acid solutions, the conductivity of the solutions decreased, because glycerol just serves as a plasticizer which does not conduct electricity.[28] In addition, when the electrical conductivity was compared, it was shown that D-chitosan dissolved in acetic acid had a lower value than those of citric and malic acids. This is because acetic acid is monocarboxylic, resulting in weak ionization and low electrical conductivity.[29] In summary, the different viscosity and conductivity values were substantially influenced by the solution compositions.

3.1.3. Visual Appearance of the Biofilms. The appearance and color of film packaging are some of the most important factors influencing and attracting customers. As shown in Figure S2, the D-chitosan/multicarboxylic acid biofilm was glossy and smooth (Figure S2A,C,E). The visual appearance of the D-chitosan/multicarboxylic acid biofilm with glycerol was light yellow and did not change significantly from the biofilms without the plasticizer. Similar phenomena were previously explained in the literature, namely that adding a plasticizer such as soybean oil to a chitosan matrix did not change the color of the film.[30] In addition, biofilm colors did not differ significantly when analyzed using the RGB color model (Figure S2). As a result of this examination, it was discovered from this investigation that all of the biofilms had similar appearances, such as color. Additionally, each biofilm had a high-gloss surface and was free of wrinkles.

3.1.4. Mechanical Properties. Figure S3 depicts the TS values of the biofilms. According to the experiment results, biofilms had quite high TS values prior to the addition of glycerol (Figure S3A,C,E). In particular, D-chitosan/acetic acid biofilm provides TS values up to 30 MPa (Figure S3A). This

https://doi.org/10.1021/acsomega.4c01482
ACS Omega 2024, 9, 41179−41193

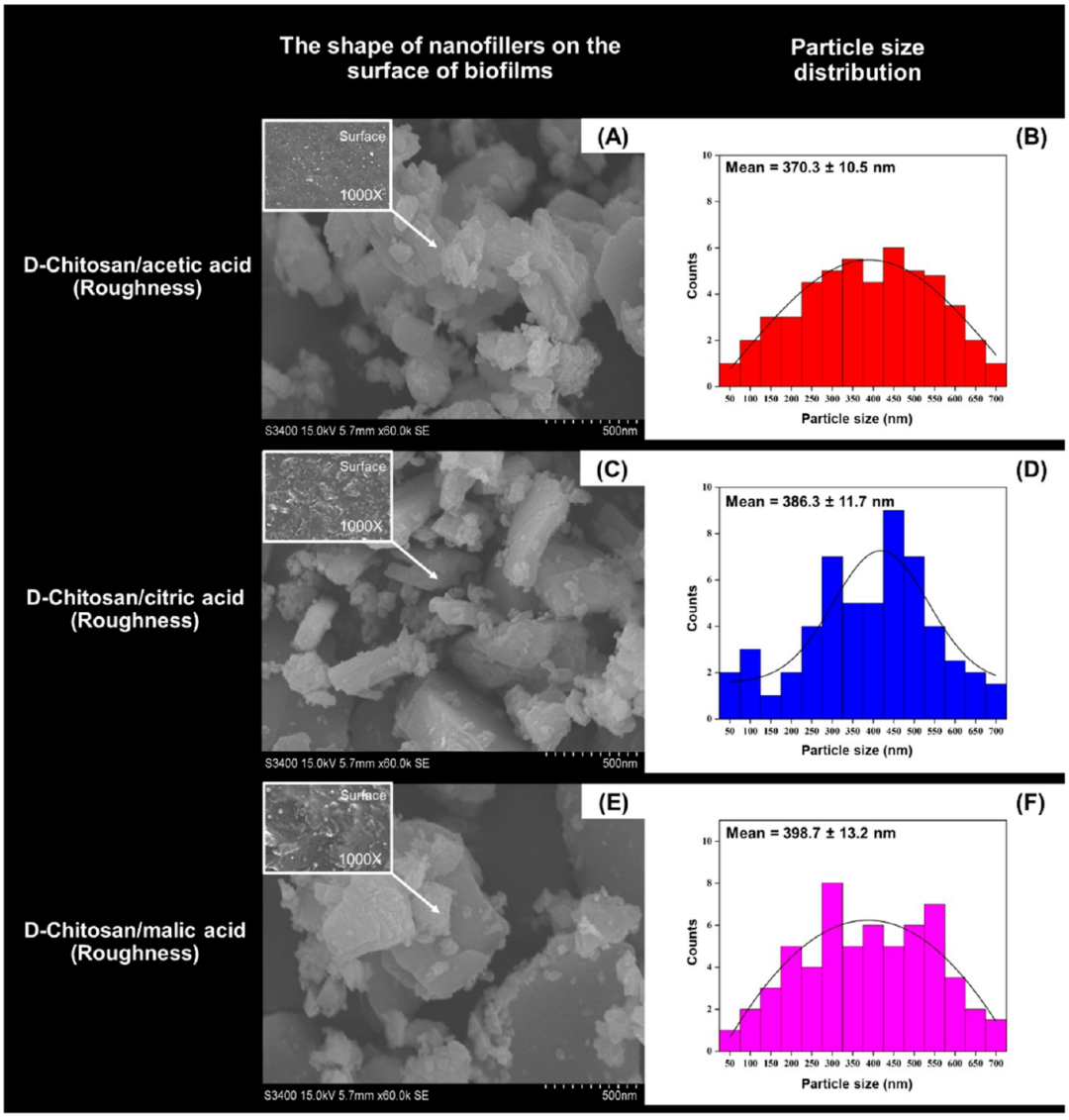

Figure 2. Shape of nanofillers on the surface of biofilms at a magnification of 60,000× and particle size distribution.

demonstrates that acetic acid is a highly effective solvent and a film-forming agent. Meanwhile, D-chitosan/citric acid biofilm appears to create high levels of TS values (Figure S3C), similar to the use of acetic acid as a biofilm-forming agent. In contrast, the TS values for the D-chitosan/malic acid biofilm were quite low (Figure S3E). As a consequence of the experimental results, it appears that the use of acetic acid as a type of monocarboxylic acid is quite suitable for biofilm formation. This could be because of the exceptional solubility of D-chitosan powder in acetic acid, which produces strong compatibility between the structure of the D-chitosan chains and the monoacid. This result becomes consistent with the comparatively low viscosity of the D-chitosan/acetic acid solution (Table 1), indicating the high solubility of D-chitosan in this acid. In addition, when glycerol was added to the biofilm structure (Figure S3B,D,F), the TS values were significantly lowered. This is because glycerol increases the free volume and mobility of the chitosan polymer chain, leading to a drop in TS values.[31] Figure S4 depicts the percentage of EB values of the biofilms. The experimental results show that the EB values before the addition of glycerol were quite low (Figure S4A,C,E). And it seems that the D-chitosan/acetic acid biofilm has the lowest value (Figure S4A). However, the EB values dramatically increased when the biofilm characteristics were enhanced by the addition of a modest amount of glycerol (Figure S4B,D,F). Glycerol interfered with D-chitosan chains, significantly reducing intermolecular liking, and increasing polymer mobility, allowing biofilms to stretch.[32] Finally, a small quantity of glycerol would be very helpful for biofilms in order to achieve optimum mechanical properties.

3.1.5. Morphology of Biofilms. The morphology of the biofilms was evaluated by using SEM analysis. Figure 1 depicts the surface morphology of the biofilms. The morphology analysis showed that the surface of the biofilms before the addition of glycerol had a visible distribution of D-chitosan powder and roughness [(Figure 1A−C) (Figure 1G−I), and (Figure 1M−O)]. It is this visible residual D-chitosan powder from acid solubility that acted as a filler in the biofilms, which aids in reinforcing, particularly in the D-chitosan/acetic acid biofilm that has a relatively high TS. Besides, when the surface characteristics of the biofilms were evaluated, it was discovered that the D-chitosan/acetic acid (Figure 1A−C) biofilm had a relatively good surface nanosized-fillers dispersion when compared to the D-chitosan/citric acid (Figure 1G−I) and D-chitosan/malic acid (Figure 1M−O) biofilms. That is why the D-

https://doi.org/10.1021/acsomega.4c01482
ACS Omega 2024, 9, 41179−41193

chitosan/acetic acid biofilm has an exceptional TS. When glycerol was added to biofilms in Figure 1, the nanofillers on the surface of the biofilms became more distributed to the extent that they were nearly homogeneous with the biofilms [(Figure 1D−F) (Figure 1J−L), and (Figure 1P−R)]. This demonstrates that glycerol could function as a dispersant agent in addition to being a plasticizer. Therefore, adding glycerol into the structure of biofilms will not only help to smoothen the biofilms but also increase their mechanical performance and flexibility. When SEM cross section was performed, the sample showed a similar trend as illustrated in Figures S12 and S13. Additionally, the AFM analysis also confirmed that the film's surface was very smooth with slight roughness at nanometer length scale, as shown in Figure S16. In summary, the appropriate addition of glycerol was helpful for biofilms, particularly in terms of the smoothness and usability.

Furthermore, the morphology of the nanofillers was further evaluated by direct observation of their physical size, shape, and orientation under SEM. As shown in Figure 2, the nanofillers found in the D-chitosan/acetic acid film were sheet-like, aggregated (Figure 2A), with a particle size of 370.3 ± 10.5 nm (Figure 2B). The nanofillers in the D-chitosan/citric acid film had more rod than sheet characteristics (Figure 2C) and a particle size of 386.3 ± 11.7 nm (Figure 2D) when measured. When the nanofillers in the D-chitosan/malic acid film were analyzed, they revealed a dense overlapping sheet shape (Figure 2E) distinct from that of the nanofillers observed in other biofilms. Finally, when the particle size was measured, it was found to be quite large, ranging between 398.7 ± 13.2 nm (Figure 2F). Additionally, an in-depth study revealed that the nanofillers' small particle sizes resulted in significant differences in TS. It was discovered that the smallest nanoparticles in D-chitosan/acetic acid provided the highest TS. More importantly, it appears that the viscosity solution of the D-chitosan/acetic acid film has the lowest viscosity, which is likely due to the acid dissolving the nanofillers until the particle size is small.

3.1.6. FT-IR Analysis. To investigate the interaction of D-chitosan and multicarboxylic acid, FT-IR tests were performed on D-chitosan biofilms cast from different acid solutions. Figure 3 depicts the FT-IR spectra of D-chitosan powder (Figure 3A) and biofilms (Figure 3B−G). For all the samples, the broad absorption band between 3400 cm^{-1} is assigned to the stretching of hydrogen bonded hydroxyl groups of the carbohydrate ring.[33]

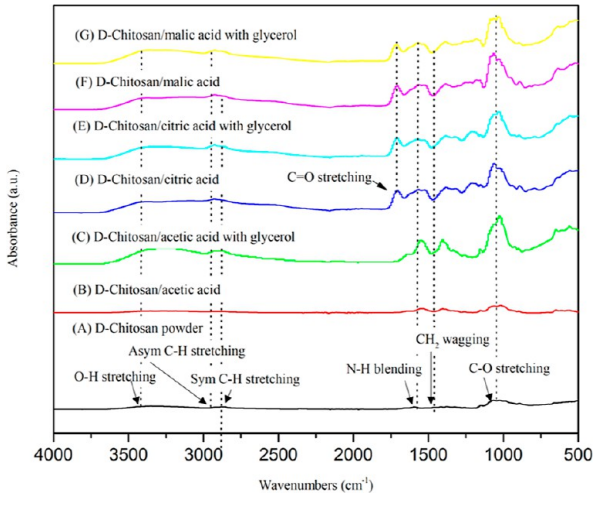

Figure 3. FT-IR spectra of D-chitosan powder and biofilms.

The absorption bands at 2900 cm^{-1} (asymmetric C−H stretching) and 2800 cm^{-1} (symmetric C−H stretching) indicate the functional group that is the primary component of D-chitosan.[33] While the absorption bands at 1550 cm^{-1} (N−H bending vibrations of $NHCOCH_3$ group (Amide II), 1370 cm^{-1} (vibration of C−H bending in the ring), and 1050 cm^{-1} (skeletal vibrations involving the C−O stretching) of the D-chitosan polysaccharide structure were also observed in the D-chitosan powder and biofilms.[33] The main differences in D-chitosan powder and biofilms were found in the medium infrared region at ∼1700 cm^{-1}, where the characteristic band of carbonyl (C═O) at 1693 cm^{-1} related to the carbonyl stretch C═O of citric and malic acids in D-chitosan/citric and D-chitosan/malic acid biofilms,[34] which are not found in D-chitosan powder. In contrast, the D-chitosan/acetic acid biofilm was found to be strongly shifted from 1693 to 1673 cm^{-1} at the carbonyl (C═O) position, indicating strong hydrogen bonding. As a result, D-chitosan/acetic acid biofilm may possess properties that set them above other biofilms. The addition of glycerol in the formulation had no effect on the FT-IR spectra (Figure 3C−E), indicating that these additives have no effect on the chemical structure of chitosan. Furthermore, the fact that the FT-IR spectra were unaffected by the addition of glycerol indicated that no new types of bonds were formed. However, there could have been differences in the intensities of existing bonds. This is not very significant in the structures of biofilms.

3.1.7. Crystalline Structure. Figure 4 depicts the diffractograms of the D-chitosan powder and biofilms. The XRD pattern

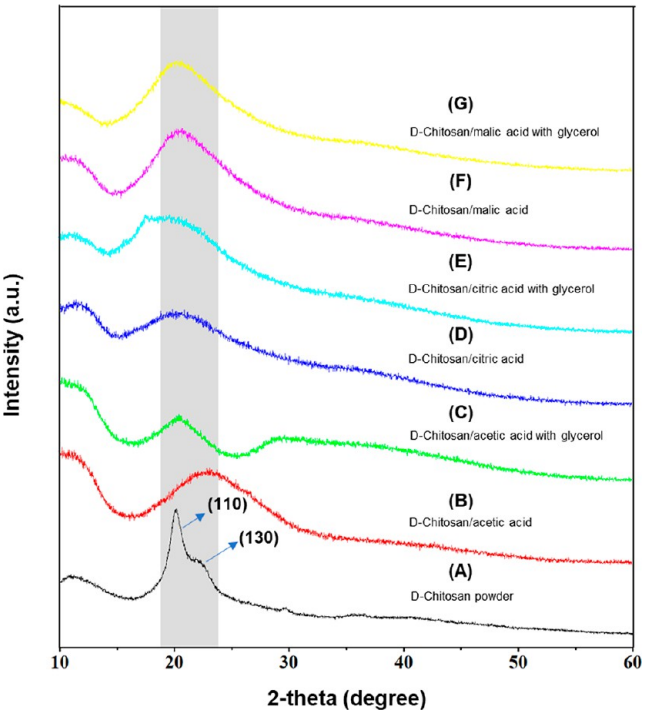

Figure 4. XRD patterns of the D-chitosan powder and biofilms.

of D-chitosan powder showed two major peaks at (110) and (130) planes (Figure 4A), as well as a relatively broad peak at around 2-theta = 20°, indicating that it is semiamorphous. This corresponds to previous research.[35] All biofilms showed a combination of characteristic peaks. The combination of D-chitosan and multicarboxylic acid decreased crystallinity, as evidenced by broad peaks in the XRD patterns (Figure 4B−G).

https://doi.org/10.1021/acsomega.4c01482
ACS Omega 2024, 9, 41179−41193

Table 2. Crystallinity Index (CI %), Crystallite Size (nm), Percentage of Swelling, OP, Thickness, and Antibacterial Property of Biofilm from Chitosan in Bioacid

samples	crystallinity (CI %)	crystallite size (nm)	swelling (%)	OP (cm^3 μm m^{-2} day^{-1} kPa^{-1})[a]	thickness (mm)[b]	bacterial reduction (%)	
						S. aureus	K. pneumoniae
D-chitosan powder (control)	81.77	2.09	N/A	N/A	N/A	>99.90	99.52
D-chitosan/acetic acid	63.21	0.63	82	7.42 ± 0.13	0.51 ± 0.12	>99.90	>99.95
D-chitosan/acetic acid with glycerol	70.73	0.69	90	7.61 ± 0.24	0.56 ± 0.14	>99.90	>99.95
D-chitosan/citric acid	51.02	0.52	85	7.68 ± 0.17	0.52 ± 0.16	>99.90	>99.95
D-chitosan/citric acid with glycerol	57.72	0.60	93	7.97 ± 0.28	0.57 ± 0.13	>99.90	>99.95
D-chitosan/malic acid	62.23	0.72	96	9.82 ± 0.46	0.55 ± 0.12	>99.90	>99.95
D-chitosan/malic acid with glycerol	69.23	0.73	102	10.94 ± 0.48	0.58 ± 0.11	>99.90	>99.95

[a]Mean of three replicates ± standard deviations. [b]Mean of six replicates ± standard deviations.

This result is quite consistent with the crystallinity index in Table 2. However, when the XRD pattern was considered, the D-chitosan/acetic acid (Figure 4B) biofilm exhibits a slightly more right-shifted pattern than the biofilms formed with citric acids (Figure 4D) and malic acids (Figure 4F). And this may be the cause of the outstanding qualities of acetic acid-based biofilm, particularly their remarkable TS. When glycerol was added to the film structure, the XRD pattern did not change significantly where the main peak remained in the same position (Figures 4C,E,G). This suggests that glycerol functions just as a plasticizer and does not change the internal chemical structure of the biofilms. As the percentage of crystallinity and crystallite size of biofilms were calculated (Table 2), they were significantly lower than with D-chitosan powder (control). This means that the multicarboxylic acids used to produce the biofilms dissolve the crystalline of D-chitosan powder, affecting the percentage of crystallinity and crystallite size.[36] The dissolution of the crystalline in D-chitosan powder causes the polymer chains in D-chitosan to be more easily displaced, resulting in the formation of a solution capable of creating biofilms. Once the percentage of crystallinity and crystallite size of biofilms were analyzed, it was discovered that the D-chitosan/acetic acid biofilm had a slightly higher level of crystallinity than the D-chitosan/citric acid and D-chitosan/malic acid biofilms. This characteristic is expected to result in the D-chitosan/acetic acid biofilm having superior physical properties to other biofilm formulations, particularly giving the highest TS and water contact angle while having the lowest swelling percentage. The percentages of crystallinity and crystallite size increased when glycerol was added to the structure of the biofilms. This is likely because glycerol enables the polymer chains in D-chitosan to move freely, resulting in an improved crystal arrangement.[37] In conclusion, XRD analysis shows that biofilms still have some crystallinity, which influences their characteristics.

3.1.8. Swelling Properties. One of the most important parameters influencing the biofilm is the percentage of swelling because biofilm requires exposure to moisture or water in the environment. Table 2 displays a quantitative examination of the percentage of swelling, demonstrating that all of the biofilms swell for about 82−102% in deionized water (pH = 7.12) without disintegration, indicating the presence of a unique high-strength structure as well as hydrophobic characteristics.[38] According to the findings, the D-chitosan/acetic acid biofilm exhibited a lower percentage of swelling than did the D-chitosan/citric acid and D-chitosan/malic acid biofilms. This demonstrates that the internal structure of D-chitosan biofilms is different, particularly D-chitosan biofilms produced from acetic acid. It is anticipated that the usage of acetic acid, a monocarboxylic acid, in film formation will differ in its chemical structure form. This result is somewhat compatible with the FT-IR results (Figure 3), indicating that the C═O stretching group in D-chitosan/acetic biofilms is more shifted, making this functional group less visible and thus affecting the chemical structure directly. Whereas biofilms from D-chitosan/citric acid and D-chitosan/malic acid biofilms obviously peaked in the C═O stretching group. As a result, there is less water absorption, which leads to reduced swelling. Therefore, the biofilms made from acetic acid have less water absorption, causing less swelling. Nevertheless, when glycerol is added to the structure of the biofilms, the swelling values of the biofilms are greatly raised because the OH group of glycerol enhances the biofilms' ability to absorb more water, leading to higher swelling of the biofilms.[39] In summary, the percentage of swelling varies depending on the acid that forms the biofilms. This qualifies biofilms for a wide range of applications, particularly for single-use and degradable food packaging with a low environmental impact.

3.1.9. Contact Angle Properties. The contact angles of the biofilms could be strongly related to how the biofilm might behave upon exposure to water. The contact angles of various biofilms are shown in Figure S5. As illustrated, the highest contact angle before adding glycerol is from the D-chitosan/acetic acid biofilm (111.4°), which is greater than both D-chitosan/citric acid (110.1°) and D-chitosan/malic acid biofilms (46.9°), as shown in Figure S5A,C,E, respectively. This implies that the D-chitosan/acetic acid biofilm is relatively more hydrophobic. This result corresponds to the effect of a low percentage of swelling (Table 2). However, the result of being the monocarboxylic acid of acetic acid is also significant, because this acid has only one OH group. It imparted in a biofilm with more hydrophobic properties than when the di- and tricarboxylic acids are used.[40] Additionally, after adding glycerol to the biofilms (Figure S5B,D,F), it was observed that biofilms had significantly low contact angle values because the glycerol makes the biofilms more hydrophilic. All of the above shows that the acids used in biofilm production can greatly affect the hydrophilic and hydrophobic characteristics of the biofilms.

3.1.10. OP Properties. The appropriate OP values determine the films' usage in each application since OP values are crucial in film packaging. Table 2 shows the OP values of the biofilms. D-chitosan/multicarboxylic acid biofilms had OP values that ranged from 7.42 to 10.94 cm^3 μm m^{-2} day^{-1} kPa^{-1}. That was an

https://doi.org/10.1021/acsomega.4c01482
ACS Omega 2024, 9, 41179−41193

excellent level for OP values as the value were around 10 μm m^{-2} day^{-1} kPa^{-1} or less.[49] However, a further comparison of the OP values reveals that the D-chitosan/acetic acid biofilm offers the lowest OP values (7.42 ± 0.13 cm^3 μm m^{-2} day^{-1} kPa^{-1}). This indicates that the structure inside the film has a relatively high intermolecular density, making oxygen gas difficult to pass through. This corresponds to the fact that the D-chitosan/acetic acid biofilm has the highest TS and a high level of percentage of crystallinity. When it came to film thickness (Table 2), it was discovered that the thicknesses were so similar that they did not significantly differ substantially. Therefore, it is not regarded as a relevant factor in comparing the OP values. Also, once the characteristics of biofilms were improved to make them more flexible by adding glycerol, the OP values increased considerably. Because glycerol was utilized as a plasticizer, the polymer chains in the biofilms structure moved more easily, resulting in increased OP diffusion.[41] In addition, the OP properties have also caused all of the results mentioned above to be correlated to the surface morphology. It was noted that the surface of the film had a roughness before the addition of glycerol, resulting in low OP values due to the presence of D-chitosan powder in the form of nanofillers remaining from the dissolution. In contrast, glycerol improved the dispersion of nanofillers in the biofilms, giving them a smoother surface. As a result, the gas permeability to oxygen was improved.

3.1.11. Antibacterial against. The antibacterial property of packaging is important in modern environment. Therefore, this standard should also be present in modern packaging film. Table 2 shows the antibacterial activity of D-chitosan powder (control) and biofilms. When biofilms are compared to D-chitosan powder, the bacterial reduction is not significantly different, especially for *S. aureus*. This means that D-chitosan in both powder and biofilm forms was antibacterial. The combination of D-chitosan/multicarboxylic acid biofilms improved the bacterial reduction to 99.95% of *K. pneumoniae*. This reason is expected to be due to the fact that multicarboxylic acid can increase positive charge, which improves antibacterial against.[42] Interestingly, adding glycerol to the biofilms had no effect on the bacterial reduction. In conclusion, all D-chitosan powders and biofilms are resistant to bacterial reduction by up to 99.50%. Finally, the positive qualities of biofilms render them appropriate for use in the food packaging industry, especially in preserving food against a broad microbial spectrum.

3.1.12. Food Preservation Application. In tropical areas such as Thailand, the Cavendish banana is a widely popular fruit because it gives both energy and nutrients. However, this type of banana has the disadvantage of decaying quickly and cannot be stored for a long period of time, typically for only 4 days. In order to demonstrate an impactful application, the produced biofilms were tested on Cavendish bananas in this research to see if the shelf life could be extended. At room temperature test under normal conditions, Figure S6, revealed that at day 0, the outside skins of all unwrapped bananas were bright yellow (Figure S6A−G). When whole bananas were wrapped under biofilms (Figure S6B−G), the outside skin of the bananas changed slightly on day 2, with the appearance of black spots. After day 4, the biofilms were still effective at prolonging the decay of the bananas with a minor change on the banana outside skin compared to day 2. The outside skin of the banana changed significantly by day 6 with the appearance and expansion of black spots. On day 8, the banana skin had large black spots and scars from decaying and a slight unpleasant odor. Based on the experimental results, it is possible to conclude that the biofilms obtained from this research have a high ability to delay food decay. It was also found that the efficiency of biofilms in each formulation in prolonging the banana shelf life was not significantly different.

3.1.13. Visual Appearance of the D-Chitosan Film-Forming Solution. As summarized in Table 3, the film-forming solution was prepared at a low temperature (Figure S7). This leads to relatively low energy use during the process, which is a beneficial thing. While the D-chitosan solution was stirred with other components, a large number of foams are formed. When this solution is cooled to room temperature, the foam will immediately disappear. As a result, the color of the solution could be apparent. Figure S8 showed the experimental results, D-chitosan/SA (Figure S8A) was transparent, and when glycerol was added (Figure S8B), the color of the solution did not change. Because glycerol is a clear, colorless solution, it does not discolor the D-chitosan/SA. When CNC is added to the D-chitosan/SA (Figure S8C,D), the solution color changes to a milky color because CNC is a white powder. Therefore, the color of the solution affects the film.

Table 3. Viscosity and Conductivity of D-Chitosan in SA at 25 °C

solutions	solution properties	
	viscosity (cP)[a]	conductivity (μS/cm)[a]
SA (control)	8.12 ± 0.34	1237.56 ± 6.00
SA/glycerol	40.86 ± 2.31	1217.13 ± 6.95
D-chitosan/SA	257.38 ± 4.26	3010.83 ± 13.26
D-chitosan/SA with glycerol	280.21 ± 4.55	2961.47 ± 5.83
D-chitosan/SA/CNC	372.33 ± 5.28	3084.80 ± 1.82
D-chitosan/SA/CNC with glycerol	410.25 ± 6.27	3018.90 ± 13.37

[a]Mean of three replicates ± standard deviations.

3.1.14. Solution Properties. The viscosity and conductivity of the D-chitosan powder dissolved in SA and combined with other components would be analyzed. These two parameters are important because they affect film formability, as well as bacterial resistance. Table 3 shows the viscosity and conductivity of the D-chitosan solutions with varying compositions. The viscosity of D-chitosan/SA is 257.38 ± 4.26 cP (Table 3), which is a high viscosity value when compared to SA (control) and SA/glycerol. This revealed that D-chitosan polymer chain-to-chain interaction or entanglement was present in the SA solution. The viscosity of the solution increased considerably when glycerol or CNC were added. This is due to the interaction of the polymer chain of D-chitosan with glycerol as well as the CNC, which causes the solution to network in the structure.[26] As a result, the solution became viscous enough to form a film. The conductivity of D-chitosan/SA is 3010.83 ± 13.26 μS/cm. It is higher than that of SA (control) and SA/glycerol. This meant that the increase in conductivity could well be attributed to increased amounts of free ions (both positive and negative ions).[27] This could be assumed to be caused by the dissociation of NH_3^+ and COO^- in solution by D-chitosan and SA. It was also discovered that when CNC was added to D-chitosan/SA, the conductivity increased significantly. The increased conductivity is due to the fact that protons on the CNC surface can easily migrate and ionize.[43] In contrast, when glycerol was added to the solution, the conductivity decreased across the board because glycerol cannot be divided and conduct electricity.[28] Another reason could be that glycerol makes it difficult for protons to migrate. As a result, the electrical conductivity of the solution decreases. In summary,

https://doi.org/10.1021/acsomega.4c01482
ACS Omega 2024, 9, 41179−41193

Table 4. TS, EB, Percentage of Swelling, OP, Thickness, and Antibacterial Property of Biofilm from Chitosan in SA

samples	tensile strength (MPa)[a]	elongation at break (%)[a]	swelling (%)	OP (cm^3 μm m^{-2} day^{-1} kPa^{-1})[b]	thickness (mm)[c]	bacterial reduction (%)	
						S. aureus	K. pneumoniae
D-chitosan powder (control)	N/A	N/A	N/A	N/A	N/A	>99.90	99.52
D-chitosan/SA	5.60 ± 1.37	4.62 ± 1.16	52	7.42 ± 0.23	0.64 ± 0.14	>99.90	>99.95
D-chitosan/SA with glycerol	4.02 ± 1.20	19.03 ± 4.51	79	7.95 ± 0.45	0.66 ± 0.11	>99.90	>99.95
D-chitosan/SA/CNC	9.59 ± 1.46	2.81 ± 1.03	92	4.54 ± 0.37	0.68 ± 0.14	>99.90	>99.95
D-chitosan/SA/CNC with glycerol	8.22 ± 1.41	16.04 ± 2.17	95	4.82 ± 0.48	0.68 ± 0.18	>99.90	>99.95

[a]Mean of ten replicates ± standard deviations. [b]Mean of three replicates ± standard deviations. [c]Mean of six replicates ± standard deviations.

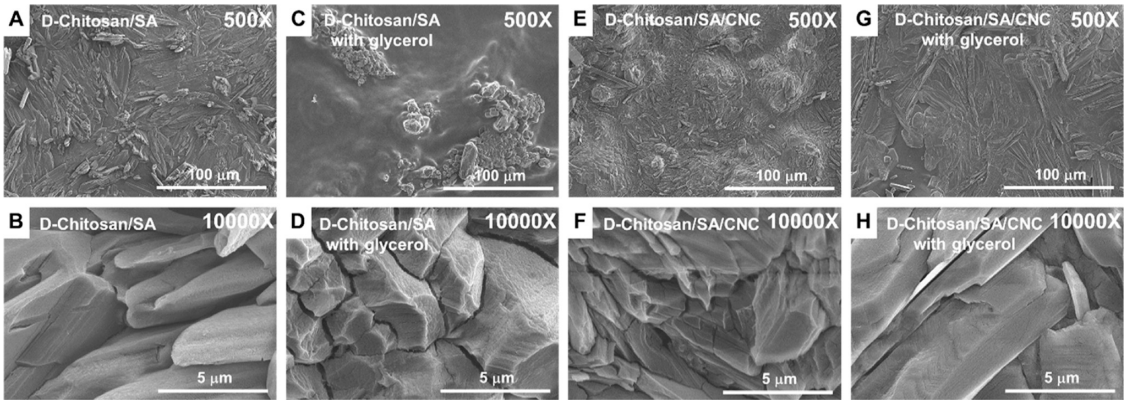

Figure 5. Morphology of biocomposite films with magnifications of 500× and 10,000×.

differing viscosity and conductivity values may have an impact on the film formability and bacterial resistance.

3.1.15. Visual Appearance of the Biocomposite Films. The color of the packaging film is critical since it affects storage and user satisfaction. Therefore, the attractive color of the packaging film will make the film more useful and have a direct effect on the growth of the packaging industry. Figure S9 depicts the characteristics of biocomposite films and the RGB color model, the D-chitosan/SA (Figure S9A) was glossy, smooth, and yellow. And there was no visible color change when glycerol was added to the biocomposite film (Figure S9B). On the contrary, when CNC was added to the biocomposite film, the color of the biocomposite film was changed to dark yellow (Figure S9C,D), because the CNC nanofiller distributes well on the surface of the biocomposite film, the color is dark. Previous literature reports explained a similar phenomenon, namely that adding cellulose to the chitosan matrix changed the color of the film.[30] In conclusion, the overall biocomposite film is relatively smooth and reflects light well without air bubbles.

3.1.16. Mechanical Properties. Table 4 shows the TS and percentage EB values of biocomposite films, respectively. The TS value for D-chitosan/SA was 5.60 ± 1.37 MPa. When glycerol was added, the TS value dropped considerably due to the plasticizer. However, the TS value for the biocomposite film with CNC added was significantly higher (9.59 ± 1.46 MPa). It demonstrates that the CNC-polymer has been well blended, especially around the interphase. The EB value was observed to decrease with the addition of CNC due to the harder biocomposite film. Furthermore, the appearance of glycerol in the biocomposite film resulted in significant changes in the TS and EB values. In other words, glycerol decreased TS while increasing EB values (Table 4). Glycerol interfered with D-chitosan chains, significantly reducing intermolecular linking and increasing polymer chain mobility, allowing biocomposite film to stretch.[31] Finally, D-chitosan/SA/CNC with glycerol addition was appropriate and beneficial for use because it has the proper degree of strength and flexibility.

3.1.17. Morphology Properties. The morphology of the biocomposite films was evaluated by using SEM analysis. Figure 5 depicts the surface morphology of the biocomposite films. The surface morphology of the D-chitosan/SA was rough, as shown in Figure 5A,B. Similarly, as shown in Figure 5C,D, adding glycerol to a D-chitosan/SA had no influence on surface roughness. Furthermore, when CNC was added to D-chitosan/SA, there was no apparent change in the surface of the film. As illustrated in Figure 5E,F, adding CNC to the D-chitosan/SA significantly roughens the surface. Moreover, the addition of glycerol to D-chitosan/SA/CNC did not result in a significant difference in surface (Figure 5G,H). In short, the addition of fillers to the biocomposite film results in a rougher surface. The morphology of the biocomposite films demonstrated a strong adhesion between the polymer matrix and the reinforcing filler. This result corresponded to an increase in TS (Table 4). All of the evidence presented above supported the conclusion that D-chitosan/SA incorporating CNC was the best film due to its higher TS properties, which are suitable for the production of packaging film.

3.1.18. Optical Microscope Analysis. The optical microscope was used to analyze the crystallinity of biocomposite films. The surface crystallinity of biocomposite films was recorded with the microcapture program shown in Figure S10. Images taken using an optical microscope clearly reveal that biocomposite films were quite a crystal and reflected light well. This is expected to be the result of high crystalline SA and CNC. When considering the D-chitosan/SA (Figure S10A), the crystal size seems fairly large, allowing the crystals to be clearly visible. When glycerol and CNC were added to the D-chitosan/SA (Figure S10B–D), the crystal size was dramatically reduced.

https://doi.org/10.1021/acsomega.4c01482
ACS Omega 2024, 9, 41179−41193

Due to the extensively distributed glycerol and CNC in the D-chitosan matrix, small crystals are generated. Finally, the optical microscopy analysis clearly shows crystals in biocomposite films.

3.1.19. FT-IR Analysis. Figure 6 depicts the FT-IR spectra of D-chitosan powder, SA, CNC, and biocomposite films. The

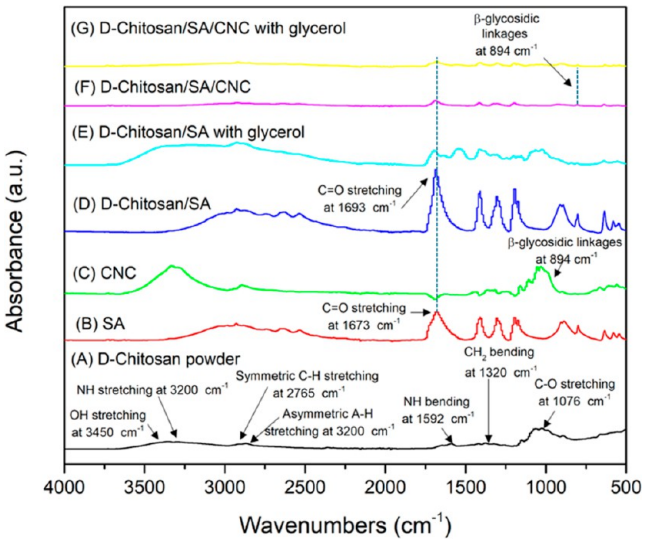

Figure 6. FTIR spectral of D-chitosan powder, SA, CNC, and biocomposite films.

stretching vibration of O−H overlapped on the N−H stretching caused D-chitosan powder (Figure 6A) and biocomposite films (Figures 6D−G) to have a broad infrared absorbance of about 3450−3200 cm^{-1}.[24] The absorption bands at 1592 cm^{-1} (N−H bending vibrations of $NHCOCH_3$ group (Amide II), 1320 cm^{-1} (vibration of C−H bending in the ring), and 1076 cm^{-1} (skeletal vibrations involving the C−O stretching) of the chitosan polysaccharide structure were also observed in the D-chitosan powder and biocomposite films.[24] The main differences in biocomposite films were found in the medium infrared region between 1200 and 1700 cm^{-1}, where the characteristic bands of carbonyl (C═O) at 1693 cm^{-1} were related to the carbonyl stretch C═O of SA (Figure 6B). The intensity of the band of carbonyl groups of SA at 1673 cm^{-1} shifted significantly to 1693 cm^{-1}, indicating the structural evidence of cross-linking between chitosan and the acid.[24] The addition of glycerol in the biocomposite films had no effect on the FT-IR spectra, indicating that the additive had no effect on the chemical structure of chitosan. Furthermore, the fact that the FT-IR spectra were unaffected by the addition of glycerol indicated that no new types of bonds were formed. However, there could have been differences in the intensity of existing bonds. When CNC was added to the D-chitosan/SA biocomposite films (Figure 6F,G), the FT-IR spectra at 894 cm^{-1} demonstrated the CNC structure's β-glycosidic linkages bond, with no shift when compared to pure CNC (Figure 6C). This implies that there was no interaction between the chitosan structure and CNC.[44] However, the addition of CNC has a significant impact on the mechanical strength of biocomposite films, despite these physical blending.

3.1.20. Crystalline Structure. Figure 7 depicts the diffractograms of D-chitosan powder, SA, CNC, and biocomposite films. The XRD pattern of D-chitosan powder (Figure 7A) showed two major peaks at (110) and (130) planes, as well as a relatively broad peak at around 2-theta = 20°, indicating that it is

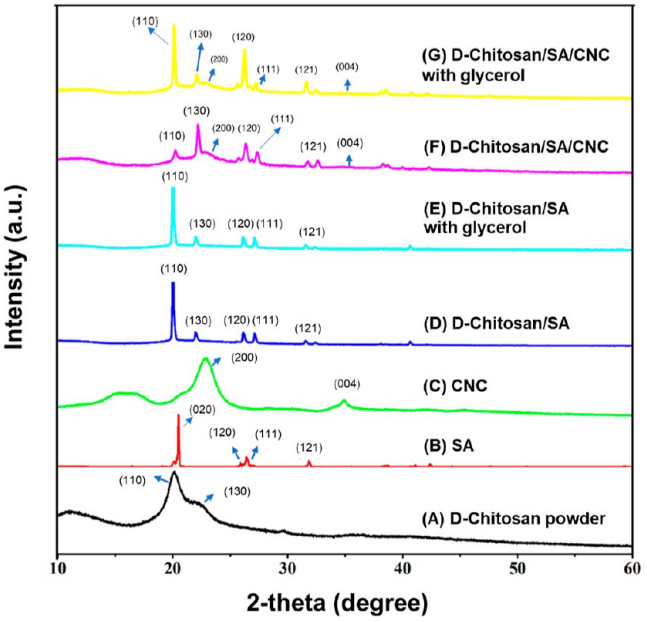

Figure 7. XRD patterns of D-chitosan powder, SA, CNC, and biocomposite films.

semiamorphous.[45] SA (Figure 7B) had a significant peak at (020), (120), (111), and (121) planes.[46] CNC (Figure 7C) displayed the typical crystalline cellulose I peaks at (200) and (004) planes, which is consistent with previous research.[15] All biocomposite films (Figure 7D−G) showed a combination characteristic peak after being blended with D-chitosan/SA. The combination of D-chitosan and SA increased crystallinity (Figure 7D,E), as evidenced by sharp peaks in the XRD patterns, which improved the mechanical strength of the biocomposite films. Furthermore, the SA peak at (020) plane disappeared due to complete overlap with the D-chitosan main peak, which corresponds to previous research.[15] The crystalline structure of CNC was quite well integrated and preserved when it was added to D-chitosan/SA (Figure 7F,G). There were no noticeable changes in the crystallinity of the biocomposite films when glycerol was added to the formulations since all major peaks remained unchanged. Therefore, glycerol acts as a plasticizer without altering the crystal structure of biocomposite films, resulting in a more flexible film. To summarize, the crystallinity of biocomposite films may be related to morphology characteristics, optical microscope images, and TS.

3.1.21. Swelling Properties. The swelling properties of packaging are a significant consideration, because the packaging must be exposed to humidity or water in the environment. Table 4 displays a quantitative examination of the percentage of swelling, demonstrating that all of the biocomposite films swelled for about 52−95% in deionized water (pH = 7.12) without disintegration, confirming the presence of a specific cross-link network. These findings show that SA can act as effective cross-linkers and generate crystallinity.[24] The incorporation of glycerol and CNC into the matrix of biocomposite films could increase the percentage of swelling (Table 4) when compared to neat D-chitosan/SA. With the addition of glycerol and CNC, the hydroxyl groups (OH^-) in glycerol and CNC could absorb more H_2O molecules, increasing the percentage of swelling ability and hydrophilic characteristics of biocomposite films.[39,47] However, when compared to monocarboxylic acids like acetic acid, cross-linking with SA resulted in a lower

https://doi.org/10.1021/acsomega.4c01482
ACS Omega 2024, 9, 41179−41193

percentage of swelling.[48] This meant that the amino acid group in D-chitosan cross-linked SA more effectively, which resulted in less swelling for water absorption. In summary, SA can function as a film-forming solvent as well as a cross-linker agent.

3.1.22. Contact Angle Properties. The contact angles of the biocomposite films are highly interesting because they will help us understand how the biocomposite films behave when exposed to water. Figure S11 shows the contact angles of various biocomposite films. The contact angle of D-chitosan/SA (Figure S11A), D-chitosan/SA with glycerol (Figure S11B), D-chitosan/SA/CNC (Figure S11C), and D-chitosan/SA/CNC with glycerol (Figure S11D) were 85.4, 64.5, 62.1, and 58.2°, respectively. The high contact angle (85.4°) of the D-chitosan/SA (Figure S11A) could be attributed to the hydrophobic main chains of the D-chitosan chains as well as the effect of intramolecular cross-linking. This resulted in a dense surface structure that was also hydrophobic. It was also found that the addition of glycerol and CNC considerably decreased the contact angle values of biocomposite films because the OH group in glycerol and the CNC structure were hydrophilic. Furthermore, an increase in surface roughness caused by the addition of CNC to biocomposite films may result in a decrease in contact angle values.[41] Finally, the hydrophobic and hydrophilic capabilities of the biocomposite films were affected by varying contact angle values, resulting in different film features.

3.1.23. OP Properties. The OP values are a significant aspect in estimating the potential for prolonging the shelf life of food. Table 4 shows the OP values of biocomposite films with comparable film thicknesses. D-chitosan/SA has an OP value of 7.42 ± 0.23 cm^3 μm m^{-2} day^{-1} kPa^{-1}. This OP value was likely low due to the cross-linking effect of the D-chitosan chains with SA. The addition of glycerol increased the OP values of biocomposite films because glycerol was used as a plasticizer, the chains in the D-chitosan structure moved more freely, leading to higher OP diffusion.[41] However, when CNC was added to D-chitosan/SA, the OP values dropped dramatically (4.54 ± 0.37 cm^3 μm m^{-2} day^{-1} kPa^{-1}). Morphological images clearly reveal that CNC considerably densifies the surfaces of biocomposite films. The results were linked to lower OP values. In the food packaging industry, an established threshold value for OP value is 38.9 cm^3 μm m^{-2} day^{-1} kPa^{-1} (10 cm^3 mil/100 $in.^2$ day atm), below which a material is considered a good barrier.[41] The OP values of all of the biocomposite films obtained were lower than this threshold value, showing that they are excellent barrier materials. Among all the biocomposite films tested, D-chitosan/SA/CNC showed an excellent oxygen barrier property, which is important for food packaging. In comparison to the previously reported chitosan/gallic acid/zinc films,[4] the prepared D-chitosan/SA/CNC film have a substantially stronger oxygen barrier property. As a result, the low OP values were mainly the effects of SA and CNC.

3.1.24. Antibacterial Properties. The antibacterial properties of packaging are important in the modern environment. Therefore, this standard should also be present in modern packaging films. Table 4 shows the antibacterial properties of D-chitosan powder (control) and biocomposite films. When biocomposite films were compared to D-chitosan powder, it could be noted that bacterial reduction was not significantly different, especially for *S. aureus*. This meant that D-chitosan in powder and biocomposite films formed were similarly antibacterial. The combination of D-chitosan powder with SA improved the antibacterial activity of all biocomposite films, especially against *K. pneumoniae*. This observation was expected due to the fact that SA acidity can increase positive charge, which improves antibacterial property.[42] Furthermore, the addition of glycerol and CNC to the biocomposite films had no effect on the bacterial reduction. Finally, biocomposite films have a remarkable antibacterial capability.

3.1.25. UV-Light Barrier of Biocomposite Films. The other crucial and indispensable property of the biocomposite film is the UV light barrier, because an effective UV light barrier can be utilized in a wider variety of applications, such as in the food packaging industry to help enhance food shelf life. Figure 8

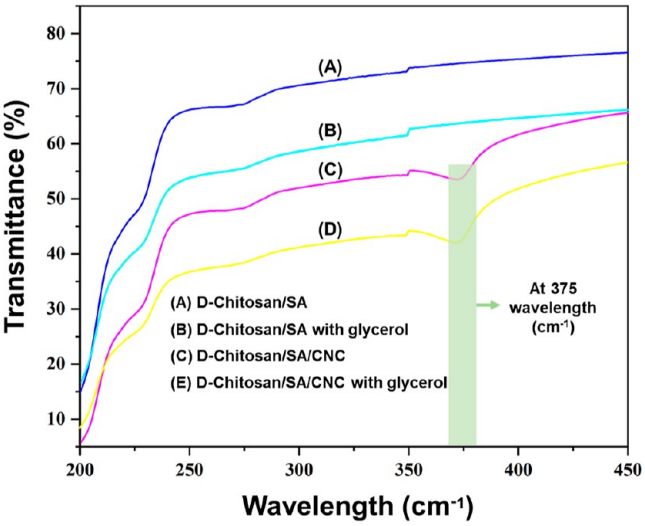

Figure 8. UV-light barrier of biocomposite films.

shows that the biocomposite film tested by a UV spectrophotometer has a decrease in light transmittance in the UV-A (320−400 nm) and UV-B (280−320 nm) ranges. This indicates that biocomposite films (Figure 8A−D) may effectively block UV light. The explanation for this is probably because the high crystallinity of the film, shown by the XRD results, decreases the UV transmittance. In addition, the bond cross-linking effect of D-chitosan and SA plays an important part in reducing UV light transmittance. When Figure 8A,B were compared, it was discovered that the addition of glycerol somewhat reduced the UV transmittance. In more detail, in Figure 8C,D, the addition of CNC significantly decreased the UV light transmittance. Particularly, the reduction in UV transmittance at 375 nm implies that CNC is crucial for the UV light barrier. In summary, biocomposite films that have CNC added to the structure perform better in terms of the UV light barrier.

3.1.26. Scheme of Biocomposite Films. From the above characterization results, it could be said that for the composite film, multiple intermolecular hydrogen bonds were formed between the −COOH group of SA and the $-NH_2$ group of D-chitosan, which led to excellent solubility and increased the stability of biocomposite films. The CNC filler had no chemical interaction with the D-chitosan/SA polymer matrix because it only acted as a physical reinforcing phase, which improved the mechanical properties of the films. The depiction of these intermolecular hydrogen bonding sites, cross-linking molecules, and CNC dispersed in the D-chitosan/SA polymer matrix is illustrated in Figure 9.

3.1.27. Film Processibility by Doctor Blade Method. The development of scalable processability was investigated under a

https://doi.org/10.1021/acsomega.4c01482
ACS Omega 2024, 9, 41179−41193

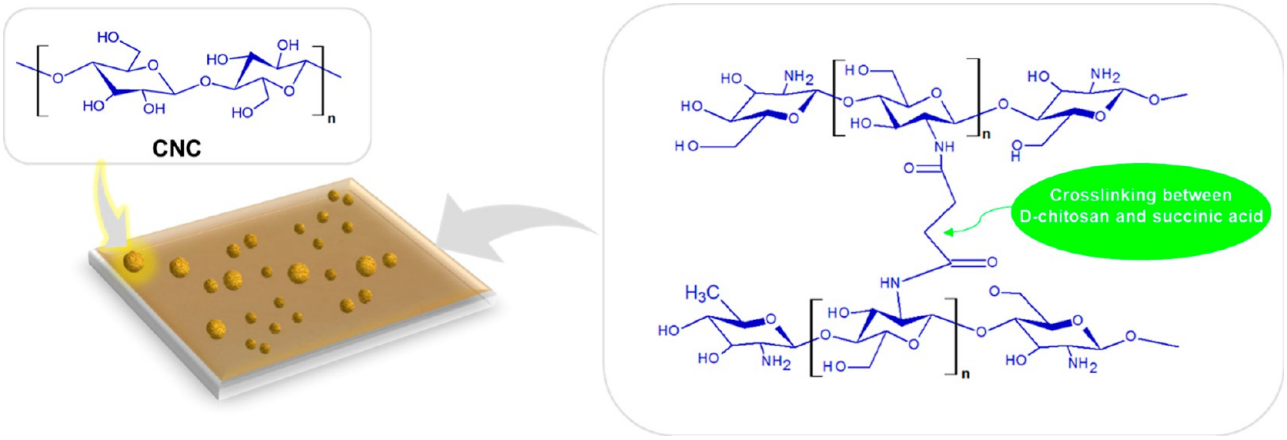

Figure 9. Summarized scheme of D-chitosan/SA incorporated CNC biocomposite films.

doctor blade as a model method which represented one of the most prevalent and versatile industrially relevant processes in film and packaging industries. Initially, we discovered that even though D-chitosan in bioacids could easily and successfully be fabricated into films via solvent casting in a static mold, the process of the same solutions under a doctor blade with dynamic casting turned out to be quite a challenge. In other words, most of the as-cast films were inhomogeneous, showing unevenness on the surface and breakage every now and then while the solutions were taken up and turned into thin films. Moreover, the respective dried films after heat-assisted evaporation of solvent were also mechanically unstable due to the high brittleness and low flexibility. It was hypothesized that the doctor blade's dynamics process might have induced in the biofilms relatively higher degree of crystallinity, the same reconstructed crystals found earlier in this study. Nevertheless, it was found also that film processability of the squid-pen's chitosan bionanocomposite could straightforwardly be compatible with and improvable in the presence of polyvinyl alcohol (PVA) employed as a model biodegradable processing aid (Figure 10). Additional analyses on physical appearance and structure such as SEM of the surface and SEM cross-sectional images of the samples are provided in Figures S14 and S15, where smooth surface and bulk structures are evident. By using AFM, a similar result was found where there was only slight roughness at nanometer length scale, as shown in Figure S17. It was noted also that the addition of PVA did not drastically change the thermal transition profiles under DSC and TGA analyses, as illustrated in Figures S18 and S19. Subsequently, from the continuity of film forming and smooth appearance of the resulted films, PVA could have acted as an excellent film forming agent and a plasticizer, adjusting the viscosity, flowability, and molecular entanglement, for desirable bionanocomposite films.

Figure 10. Bionanocomposite film by doctor blade process using PVA as a processing aid. (A) Solution of D-chitosan in bioacid with PVA, (B) film casted by doctor blade on brown paper, and (C) film on black paper printed with white letter "NANOTEC".

4. CONCLUSIONS

This research discovered that D-chitosan powder extract from squid pens has a remarkable ability to produce biofilms. First, the D-chitosan powder formed into biofilms from different acids (acetic, citric, and malic acids) showed considerably varied biofilm properties in this investigation. In particular, biofilms formed from acetic acid have properties superior to those made of other acids, such as high levels of hydrophobic behavior and TS. Importantly, it also provides an excellent level of OP values. These excellent results were obtained using the chitosan-based nanofillers that were left over after chitosan and acetic acid were dissolved. The biofilms formed from heterogeneous acids have the same high levels of antibacterial (against *S. aureus* and *K. pneumoniae*). Furthermore, when biofilms were used to wrap bananas in order to extend their freshness, it was shown that the bananas might last up to 8 days.

Second, to prepare biocomposite films, SA was used as an environmentally friendly solvent and cross-linker. The establishment of an interaction between the functional groups of chitosan and SA was demonstrated by FT-IR analysis. XRD patterns indicated that all biocomposite films had a high crystallinity, consistent with optical microscope images showing high crystallinity in biocomposite films. The addition of glycerol as a plasticizer can increase polymer chain mobility, making the biocomposite film more ductile and flexible. The addition of CNC improved the TS (41.6%), swelling (43.47%), and oxygen barrier properties (38.81%), as well as a significantly improved

https://doi.org/10.1021/acsomega.4c01482
ACS Omega 2024, 9, 41179−41193

UV light barrier of the biocomposite films. The antibacterial properties of the prepared biocomposite films were independent of the presence of glycerol or CNC. Third, the development of film processability under industrially relevant process was demonstrated by doctor blade method. It was found that film processability of the squid-pen's chitosan bionanocomposite could be compatible with and improvable in the presence of poly(vinyl alcohol), which was employed as a model biodegradable processing aid. Finally, this research demonstrated the unique potential of chitin with β-structure from the global fisher biomass waste toward industrial scalability and real-world applications of the mechanically robust and multifunctional bionanocomposite food packaging film.

■ ASSOCIATED CONTENT

Supporting Information

The Supporting Information is available free of charge at https://pubs.acs.org/doi/10.1021/acsomega.4c01482.

Section contains visual appearance of the D-chitosan film-forming solutions, the visual appearance of the biofilms and the RGB color model analysis, the TS of biofilms, the percentage of EB of biofilms, the water contact angle of biofilms, application biofilms to extend shelf life, the preparation of biocomposite films, the visual appearance of the D-chitosan film-forming solutions, the visual appearance of the biocomposite films, optical microscope images of biocomposite films at a magnification of 250×, the water contact angle of biocomposite films, SEM cross section analysis of D-chitosan/acetic acid film, SEM cross section analysis of D-chitosan/acetic acid film, SEM analysis of D-chitosan/acetic acid with PVA film, SEM cross section analysis of D-chitosan/acetic acid with PVA film, AFM of surface of D-chitosan/acetic acid and D-chitosan/acetic acid with glycerol films, AFM of surface of D-chitosan/acetic acid with PVA films, DSC of D-chitosan/acetic acid film and D-chitosan/acetic acid with PVA film, and TGA of D-chitosan/acetic acid film and D-chitosan/acetic acid with PVA film (PDF)

■ AUTHOR INFORMATION

Corresponding Author

Varol Intasanta − *The Department of Chemistry, Faculty of Science, Chulalongkorn University, Bangkok 10330, Thailand;* orcid.org/0000-0003-1636-4020; Email: varol.i@chula.ac.th

Authors

Nattapong Pinpru − *Nanohybrids and Innovation Coating (NHIC), National Nanotechnology Center (NANOTEC), National Science and Technology Development Agency (NSTDA), Khlong Luang, Pathumthani 12120, Thailand*

Chiranicha Ninthap − *Nanohybrids and Innovation Coating (NHIC), National Nanotechnology Center (NANOTEC), National Science and Technology Development Agency (NSTDA), Khlong Luang, Pathumthani 12120, Thailand*

Complete contact information is available at: https://pubs.acs.org/10.1021/acsomega.4c01482

Author Contributions

§N.P. and C.N. are first authors.

Notes

The authors declare no competing financial interest.

■ ACKNOWLEDGMENTS

This research has received funding support from the NSRF via the Program Management Unit for Human Resources & Institutional Development, Research and Innovation (PMU-B, grant number B01F640033), and from the Agricultural Research Development Agency (ARDA, grant number CRP6605030570). The authors would like to thank the National Nanotechnology Center (NANOTEC), National Science and Technology Development Agency (NSTDA) for equipment supports.

■ REFERENCES

(1) Pinpru, N.; Charoonsuk, T.; Phanasun, T.; Soponpong, M.; Bongkarn, T.; Woramongkolchai, S.; Vittayakorn, N. Double-layer Composite Film of Natural Materials and Mulch Film Application. *Chiang Mai J. Sci.* **2022**, *49* (4), 1135.

(2) Terzioğlu, P.; Güney, F.; Parın, F. N.; Şen, İ.; Tuna, S. Biowaste orange peel incorporated chitosan/polyvinyl alcohol composite films for food packaging applications. *Food Packag. Shelf Life* **2021**, *30*, 100742.

(3) Pinpru, N.; Woramongkolchai, S. Crosslinking Effects on Alginate/Carboxymethyl Cellulose Packaging Film Properties. *Chiang Mai J. Sci.* **2020**, *47* (4), 712−722.

(4) Yadav, S.; Mehrotra, G. K.; Dutta, P. K. Chitosan based ZnO nanoparticles loaded gallic-acid films for active food packaging. *Food Chem.* **2021**, *334*, 127605.

(5) Nguyen, T. T.; Thi Dao, U. T.; Thi Bui, Q. P.; Bach, G. L.; Ha Thuc, C. N.; Ha Thuc, H. Enhanced antimicrobial activities and physiochemical properties of edible film based on chitosan incorporated with Sonneratia caseolaris (L.) Engl. leaf extract. *Prog. Org. Coat.* **2020**, *140*, 105487.

(6) Haghighi, H.; Licciardello, F.; Fava, P.; Siesler, H. W.; Pulvirenti, A. Recent advances on chitosan-based films for sustainable food packaging applications. *Food Packag. Shelf Life* **2020**, *26*, 100551.

(7) Huang, Y. L.; Tsai, Y. H. Extraction of chitosan from squid pen waste by high hydrostatic pressure: Effects on physicochemical properties and antioxidant activities of chitosan. *Int. J. Biol. Macromol.* **2020**, *160*, 677−687.

(8) Van Hoa, N.; Vuong, N. T. H.; Minh, N. C.; Cuong, H. N.; Trung, T. S. Squid pen chitosan nanoparticles: small size and high antibacterial activity. *Polym. Bull.* **2021**, *78* (12), 7313−7324.

(9) Huang, C. Y.; Kuo, C. H.; Wu, C. H.; Ku, M. W.; Chen, P. W. Extraction of crude chitosans from squid (Illex argentinus) pen by a compressional puffing-pretreatment process and evaluation of their antibacterial activity. *Food Chem.* **2018**, *254*, 217−223.

(10) Huang, J.; Cheng, Z. H.; Xie, H. H.; Gong, J. Y.; Lou, J.; Ge, Q.; Wang, Y. J.; Wu, Y. F.; Liu, S. W.; Sun, P. L.; et al. Effect of quaternization degree on physiochemical and biological activities of chitosan from squid pens. *Int. J. Biol. Macromol.* **2014**, *70*, 545−550.

(11) Pangon, A.; Saesoo, S.; Saengkrit, N.; Ruktanonchai, U.; Intasanta, V. Multicarboxylic acids as environment-friendly solvents and in situ crosslinkers for chitosan/PVA nanofibers with tunable physicochemical properties and biocompatibility. *Carbohydr. Polym.* **2016**, *138*, 156−165.

(12) Dupuis, G.; Lehoux, J. Recovery of chitosan from aqueous acidic solutions by salting-out. Part 2: Use of salts of organic acids. *Carbohydr. Polym.* **2007**, *68* (2), 287−294.

(13) Velasquez-Cock, J.; Ramirez, E.; Betancourt, S.; Putaux, J. L.; Osorio, M.; Castro, C.; Ganan, P.; Zuluaga, R. Influence of the acid type in the production of chitosan films reinforced with bacterial nanocellulose. *Int. J. Biol. Macromol.* **2014**, *69*, 208−213.

(14) Brink, I.; Sipailiene, A.; Leskauskaite, D. Antimicrobial properties of chitosan and whey protein films applied on fresh cut turkey pieces. *Int. J. Biol. Macromol.* **2019**, *130*, 810−817.

(15) Costa, S. M.; Ferreira, D. P.; Teixeira, P.; Ballesteros, L. F.; Teixeira, J. A.; Fangueiro, R. Active natural-based films for food

packaging applications: The combined effect of chitosan and nanocellulose. *Int. J. Biol. Macromol.* **2021**, *177*, 241−251.
(16) Sani, I. K.; Pirsa, S.; Tağı, Ş. Preparation of chitosan/zinc oxide/Melissa officinalis essential oil nano-composite film and evaluation of physical, mechanical and antimicrobial properties by response surface method. *Polym. Test.* **2019**, *79*, 106004.
(17) Dehnad, D.; Mirzaei, H.; Emam-Djomeh, Z.; Jafari, S. M.; Dadashi, S. Thermal and antimicrobial properties of chitosan-nanocellulose films for extending shelf life of ground meat. *Carbohydr. Polym.* **2014**, *109*, 148−154.
(18) Abdelhamid, H. N.; Mathew, A. P. Cellulose−metal organic frameworks (CelloMOFs) hybrid materials and their multifaceted Applications: A review. *Coord. Chem. Rev.* **2022**, *451*, 214263.
(19) Shojaeiarani, J.; Bajwa, D. S.; Chanda, S. Cellulose nanocrystal-based composites: A review. *Compos., Part C: Open Access* **2021**, *5*, 100164.
(20) de Mesquita, J. P.; Donnici, C. L.; Teixeira, I. F.; Pereira, F. V. Bio-based nanocomposites obtained through covalent linkage between chitosan and cellulose nanocrystals. *Carbohydr. Polym.* **2012**, *90* (1), 210−217.
(21) Fernandes, S. C. M.; Freire, C. S. R.; Silvestre, A. J. D.; Pascoal Neto, C.; Gandini, A.; Berglund, L. A.; Salmén, L. Transparent chitosan films reinforced with a high content of nanofibrillated cellulose. *Carbohydr. Polym.* **2010**, *81* (2), 394−401.
(22) Huang, X. Y.; Bu, H. T.; Jiang, G. B.; Zeng, M. H. Cross-linked succinyl chitosan as an adsorbent for the removal of Methylene Blue from aqueous solution. *Int. J. Biol. Macromol.* **2011**, *49* (4), 643−651.
(23) Mitra, T.; Sailakshmi, G.; Gnanamani, A.; Mandal, A. B. Studies on Cross-linking of succinic acid with chitosan/collagen. *Mater. Res.* **2013**, *16* (4), 755−765.
(24) Gabriele, F.; Donnadio, A.; Casciola, M.; Germani, R.; Spreti, N. Ionic and covalent crosslinking in chitosan-succinic acid membranes: Effect on physicochemical properties. *Carbohydr. Polym.* **2021**, *251*, 117106.
(25) Govindaraj, P.; Abathodharanan, N.; Ravishankar, K.; Raghavachari, D. Facile preparation of biocompatible macroporous chitosan hydrogel by hydrothermal reaction of a mixture of chitosan-succinic acid-urea. *Mater. Sci. Eng., C* **2019**, *104*, 109845.
(26) Chang, X.; Hou, Y.; Liu, Q.; Hu, Z.; Xie, Q.; Shan, Y.; Li, G.; Ding, S. Physicochemical and antimicrobial properties of chitosan composite films incorporated with glycerol monolaurate and nano-TiO_2. *Food Hydrocoll.* **2021**, *119*, 106846.
(27) Li, Q.-x.; Song, B.-z.; Yang, Z.-q.; Fan, H.-l. Electrolytic conductivity behaviors and solution conformations of chitosan in different acid solutions. *Carbohydr. Polym.* **2006**, *63* (2), 272−282.
(28) de Oliveira, A. C. S.; Santos, T. A.; Ugucioni, J. C.; da Rocha, R. A.; Borges, S. V. Effect of glycerol on electrical conducting of chitosan/polyaniline blends. *J. Appl. Polym. Sci.* **2021**, *138* (42), 51249.
(29) Salazar-Brann, S. A.; Patiño-Herrera, R.; Navarrete-Damián, J.; Louvier-Hernández, J. F. Electrospinning of chitosan from different acid solutions. *AIMS Bioeng.* **2021**, *8* (1), 112−129.
(30) Kaya, M.; Khadem, S.; Cakmak, Y. S.; Mujtaba, M.; Ilk, S.; Akyuz, L.; Salaberria, A.; Labidi, J.; Abdulqadir, A. H.; Deligöz, E.; Deligöz, E. Antioxidative and antimicrobial edible chitosan films blended with stem, leaf and seed extracts of Pistacia terebinthus for active food packaging. *RSC Adv.* **2018**, *8* (8), 3941−3950.
(31) Ziani, K.; Oses, J.; Coma, V.; Maté, J. I. Effect of the presence of glycerol and Tween 20 on the chemical and physical properties of films based on chitosan with different degree of deacetylation. *LWT–Food Sci. Technol.* **2008**, *41* (10), 2159−2165.
(32) Lavorgna, M.; Piscitelli, F.; Mangiacapra, P.; Buonocore, G. G. Study of the combined effect of both clay and glycerol plasticizer on the properties of chitosan films. *Carbohydr. Polym.* **2010**, *82* (2), 291−298.
(33) Pongampai, S.; Charoonsuk, T.; Pinpru, N.; Muanghlua, R.; Vittayakorn, W.; Vittayakorn, N. High Performance Flexible Tribo/Piezoelectric Nanogenerators based on $BaTiO_3$/Chitosan Composites. *Integr. Ferroelectr.* **2022**, *223* (1), 137−151.
(34) Qiao, C.; Ma, X.; Wang, X.; Liu, L. Structure and properties of chitosan films: Effect of the type of solvent acid. *Lwt* **2021**, *135*, 109984.
(35) Pongampai, S.; Charoonsuk, T.; Pinpru, N.; Pulphol, P.; Vittayakorn, W.; Pakawanit, P.; Vittayakorn, N. Triboelectric-piezoelectric hybrid nanogenerator based on BaTiO3-Nanorods/Chitosan enhanced output performance with self-charge-pumping system. *Composites, Part B* **2021**, *208*, 108602.
(36) Zhang, W.; Jiang, Q.; Shen, J.; Gao, P.; Yu, D.; Xu, Y.; Xia, W. The role of organic acid structures in changes of physicochemical and antioxidant properties of crosslinked chitosan films. *Food Packag. Shelf Life* **2022**, *31*, 100792.
(37) Jiang, X.; Luo, Y.; Hou, L.; Zhao, Y. The Effect of glycerol on the crystalline, thermal, and tensile properties of $CaCl_2$-doped starch/PVA films. *Polym. Compos.* **2016**, *37* (11), 3191−3199.
(38) Sutharsan, J.; Boyer, C. A.; Zhao, J. Physicochemical properties of chitosan edible films incorporated with different classes of flavonoids. *Carbohydr. Polym. Technol. Appl.* **2022**, *4*, 100232.
(39) Ma, Y.; Xin, L.; Tan, H.; Fan, M.; Li, J.; Jia, Y.; Ling, Z.; Chen, Y.; Hu, X. Chitosan membrane dressings toughened by glycerol to load antibacterial drugs for wound healing. *Mater. Sci. Eng., C* **2017**, *81*, 522−531.
(40) Pavoni, J. M. F.; Luchese, C. L.; Tessaro, I. C. Impact of acid type for chitosan dissolution on the characteristics and biodegradability of cornstarch/chitosan based films. *Int. J. Biol. Macromol.* **2019**, *138*, 693−703.
(41) Luo, Y.; Pan, X.; Ling, Y.; Wang, X.; Sun, R. Facile fabrication of chitosan active film with xylan via direct immersion. *Cellulose* **2014**, *21* (3), 1873−1883.
(42) Zhong, Y.; Song, X.; Li, Y. Antimicrobial, physical and mechanical properties of kudzu starch−chitosan composite films as a function of acid solvent types. *Carbohydr. Polym.* **2011**, *84* (1), 335−342.
(43) Naseri, N.; Mathew, A. P.; Girandon, L.; Fröhlich, M.; Oksman, K. Porous electrospun nanocomposite mats based on chitosan−cellulose nanocrystals for wound dressing: effect of surface characteristics of nanocrystals. *Cellulose* **2015**, *22* (1), 521−534.
(44) Patel, D. K.; Ganguly, K.; Hexiu, J.; Dutta, S. D.; Patil, T. V.; Lim, K. T. Functionalized chitosan/spherical nanocellulose-based hydrogel with superior antibacterial efficiency for wound healing. *Carbohydr. Polym.* **2022**, *284*, 119202.
(45) Liu, C. H.; Jiang, H. T.; Wang, C. H. Fabrication and characterization of a toughened spherical chitosan adsorbent only through physical crosslinking based on mechanism of Chain Rearrangement. *RSC Adv.* **2022**, *12* (15), 9179−9185.
(46) Omwene, P. I.; Sarihan, Z. B. O.; Karagunduz, A.; Keskinler, B. Bio-based succinic acid recovery by ion exchange resins integrated with nanofiltration/reverse osmosis preceded crystallization. *Food Bioprod. Process.* **2021**, *129*, 1−9.
(47) Shrestha, P.; Sadiq, M. B.; Anal, A. K. Development of antibacterial biocomposites reinforced with cellulose nanocrystals derived from banana pseudostem. *Carbohydr. Polym. Technol. Appl.* **2021**, *2*, 100112.
(48) Chen, P.-H.; Kuo, T.-Y.; Liu, F.-H.; Hwang, Y. H.; Ho, M. H.; Wang, D. M.; Lai, J. Y.; Hsieh, H. J. Use of Dicarboxylic Acids to Improve and Diversify the Material Properties of Porous Chitosan Membranes. *J. Agric. Food Chem.* **2008**, *56*, 9015−9021.
(49) Michiels, Y.; Puyvelde, P. V.; Sels, B. Barriers and Chemistry in a Bottle: Mechanisms in Today's Oxygen Barriers for Tomorrow's Materials. *Appl. Sci.* **2017**, *7* (7), 665.

https://doi.org/10.1021/acsomega.4c01482
ACS Omega 2024, 9, 41179−41193